Isobaric–isothermal fluctuation theorem

Emil Mittag, Debra J. Searles, and Denis J. Evans

Citation: The Journal of Chemical Physics **116**, 6875 (2002); doi: 10.1063/1.1462043
View online: http://dx.doi.org/10.1063/1.1462043
View Table of Contents: http://scitation.aip.org/content/aip/journal/jcp/116/16?ver=pdfcov
Published by the AIP Publishing

ARTICLES

Isobaric–isothermal fluctuation theorem

Emil Mittag
Research School of Chemistry, Australian National University, Canberra, ACT 0200, Australia

Debra J. Searles
School of Science, Griffith University, Brisbane, Qld 4111, Australia

Denis J. Evans
Research School of Chemistry, Australian National University, Canberra ACT 0200, Australia

(Received 23 August 2001; accepted 28 January 2002)

The fluctuation theorem (FT) gives an analytical expression for the probability that in a finite nonequilibrium system observed for a finite time, the Second Law of Thermodynamics is violated. Since FT deals with fluctuations, the precise form of the theorem is dependent on the particular statistical mechanical ensemble. In the present paper we describe the application of the FT to the isothermal–isobaric ensemble. © *2002 American Institute of Physics.*
[DOI: 10.1063/1.1462043]

The fluctuation theorem (FT) gives an analytical expression for the probability that in a finite nonequilibrium system observed for a finite time, the Second Law of Thermodynamics is violated. First proposed in 1993 by Evans, Cohen, and Morriss[1] (ECM2) for an ergostatted dissipative system, the FT can be written as

$$\frac{\Pr(\overline{\Sigma}_t/k_B=A)}{\Pr(\overline{\Sigma}_t/k_B=-A)}=e^{At}. \tag{1}$$

That is, the ratio of the probability that the time averaged irreversible entropy production, $\overline{\Sigma}_t$, has a positive value Ak_B, to the probability that $\overline{\Sigma}_t=-Ak_B$, increases exponentially with time and system size since Σ is extensive. This is in agreement with the Second Law of Thermodynamics. The FT can be applied to transient time averages of the entropy production evaluated over an ensemble of transient trajectories originating from a specified initial ($t=0$) ensemble (TFT). Alternatively the initial transients can be ignored in which case (1) is applied asymptotically $t\to\infty$, to an ensemble of steady state trajectories (ESSFT). Finally, assuming the nonequilibrium steady state and the initial ensemble are ergodic, an asymptotic *dynamical* FT can be applied to finite segments along a long, single, steady state phase space trajectory (DSSFT). The FT is one of the few exact mathematical expressions that is valid for nonequilibrium systems, including those that are far from equilibrium.

Since FT deals with fluctuations, the precise form of the theorem is dependent on the statistical mechanical ensemble. Since its conception, the FT has been examined and tested in various ensembles and under various conditions. ECM2 proposed the DSSFT in 1993 for an isoenergetic trajectory. Gallavotti and Cohen clarified the proof of the DSSFT for isoenergetic trajectories in 1995 using the SRB measure.[2] The TFT and ESSFT were derived for isoenergetic trajectories taken over an initially microcanonical ensemble by Evans and Searles in 1994.[3]

A formulation of FT that can be applied to arbitrary initial ensembles and dynamics has been recently been derived[4] for which a general dissipation phase function, $\Omega(\mathbf{\Gamma})$, is defined by

$$t\overline{\Omega}_t\equiv\int_0^t ds\,\Omega(\mathbf{\Gamma}(s))=\ln\left(\frac{f(\mathbf{\Gamma}(0),0)}{f(\mathbf{\Gamma}(t),0)}\right)-\int_0^t\Lambda(\mathbf{\Gamma}(s)). \tag{2}$$

Here $f(\mathbf{\Gamma}(0),0)$ is the phase space distribution function which characterizes the initial ensemble and $\Lambda(\mathbf{\Gamma})\equiv\partial/\partial\mathbf{\Gamma}\cdot\dot{\mathbf{\Gamma}}$ is the phase space compression factor. $f(\mathbf{\Gamma}(t),0)$ is the *initial* probability density evaluated at the phase point $\mathbf{\Gamma}(t)$ which is generated from $\mathbf{\Gamma}(0)$ under the *nonequilibrium dynamics*. For isoenergetic or thermostatted dynamics in the presence of a dissipative external field, the dissipation function is trivially related to the entropy production, $\Omega=\Sigma/k_B$. The general dissipation function may then be used to derive a general expression for the TFT,

$$\frac{\Pr(\overline{\Omega}_t=A)}{\Pr(\overline{\Omega}_t=-A)}=e^{At}. \tag{3}$$

The corresponding general form of the ESSFT becomes

$$\lim_{t\to\infty}\frac{1}{t}\ln\frac{\Pr(\overline{\Omega}_t=A)}{\Pr(\overline{\Omega}_t=-A)}=A \tag{4}$$

and if the nonequilibrium steady state and the initial ensemble are ergodic, Eq. (4) is the DSSFT although in this

case the probability applies to the distribution of the values of $\overline{\Omega}_t$ obtained by considering finite segments along a long, single, steady-state phase space trajectory.

Equations (3) and (4) have been used extensively in computer simulations.[4–7] Most recently Eq. (3) was applied to an adiabatic system, where $\Lambda(t)\equiv 0$ and the phase volumetherefore does not change.[6] In the present note we show that a FT can be derived for a nonequilibrium system where the initial phase space distribution is isothermal-isobaric and where the dynamics constrains the hydrostatic pressure and kinetic temperature to constant values.

Consider an N-particle system with $\mathbf{\Gamma}=(\mathbf{q},\mathbf{p})=(\mathbf{q}_1,\mathbf{q}_2,\ldots,\mathbf{q}_N,\mathbf{p}_1,\mathbf{p}_2,\ldots,\mathbf{p}_N)$ subject to a color field, F_c. The internal energy of the system is $H_0\equiv\Sigma_{i=1}^N p_i^2/2m+\Phi(\mathbf{q})=K+\Phi$, where $\Phi(\mathbf{q})$ is the potential energy; and the total Hamiltonian for the system is $H(\mathbf{\Gamma})=H_0(\mathbf{\Gamma})+F_c\Sigma_{i=1}^N c_i x_i$, where $c_i=(-1)^i$ is the color field coupling constant. Lennard-Jones units are used throughout this paper. The calculations are carried out for systems where the potential energy function is a pair potential, $\Phi(\mathbf{q})=\Sigma_{i=1}^{N-1}\Sigma_{j>i}^N\phi(|\mathbf{q}_i-\mathbf{q}_j|)$ and two forms are used for $\phi(\mathbf{q})$. The first is a standard Lennard-Jones potential with a cutoff radius of 3.0, $\phi(\mathbf{q})=4[q^{-12}-q^{-6}]$ when $q<3.0$ and $\phi(\mathbf{q})=0$ otherwise. The second is the SHREP potential,[8] which resembles a WCA potential but has the form $\phi(\mathbf{q})=(9-8q)^3$, when $q<1.125$ and $\phi(\mathbf{q})=0$ otherwise.

For an isobaric–isothermal ensemble the phase space is confined to constant hydrostatic pressure and kinetic energy hypersurfaces. The N-particle phase space distribution function is given by $f(\mathbf{\Gamma},V)\sim\delta(p-p_0)\,\delta(K-K_0)e^{-\beta_0(H_0+p_0V)}$, where p is the hydrostatic pressure, V is the volume of the N-particle system, p_0, K_0 are the fixed values of the pressure and kinetic energy, and β_0 is the Boltzmann factor $\beta_0=1/k_BT_0=2K_0/dN$, where d is the Cartesian dimension.

The systems we examine are brought to a steady state using both a Gaussian thermostat and barostat. At time $t=0$, a color field is applied and the response of the system is monitored for a time, t, that is referred to as the length of the trajectory segment. The equations of motion used are

$$\dot{\mathbf{q}}_i=\frac{\mathbf{p}_i}{m}+\dot{\varepsilon}\mathbf{q}_i,$$

$$\dot{\mathbf{p}}_i=\mathbf{F}_i-\mathbf{i}c_iF_c-\dot{\varepsilon}\mathbf{p}_i-\alpha\mathbf{p}_i, \tag{5}$$

$$\dot{V}=dV\dot{\varepsilon},$$

where

$$\mathbf{F}_i=-\frac{\partial\Phi(\mathbf{q})}{\partial\mathbf{q}_i},\quad \dot{\varepsilon}=-\frac{\frac{1}{2m}\sum_{i\neq j}\mathbf{q}_{ij}\cdot\mathbf{p}_{ij}\left(\phi''_{ij}+\frac{\phi'_{ij}}{q_{ij}}\right)}{\frac{1}{2}\sum_{i\neq j}q_{ij}^2\left(\phi''_{ij}+\frac{\phi'_{ij}}{q_{ij}}\right)+9pV}$$

is the *dilation rate*[9] and

$$\alpha=-\dot{\varepsilon}+\frac{\sum_{i=1}^N(\mathbf{F}_i-\mathbf{i}c_iF_c)\cdot\mathbf{p}_i}{\sum_{i=1}^N\mathbf{p}_i\cdot\mathbf{p}_i}$$

is the thermostat multiplier. For this system, the phase space compression factor is $\Lambda(t)=-dN\alpha$ and the dissipative flux, which is analogous to the electric current density, is defined as the time derivative of the enthalpy, $d(H_0+p_0V)/dt\equiv\dot{I}^{\mathrm{ad}}\equiv-JVF_c=-F_c\Sigma_{i=1}^N c_ip_{xi}$,[4] where $J=\Sigma_{i=1}^N c_ip_{xi}/V$ is the dissipative flux or the color current density. Under constant pressure conditions the rate of change of the enthalpy is equal to the rate of change of the entropy multiplied by the absolute temperature.

Using Eq. (2), the phase space distribution function of the initial ensemble $[f(\mathbf{\Gamma},V)\sim\delta(p-p_0)\,\delta(K-K_0)e^{-\beta_0(H_0+p_0V)}]$ and the phase space compression factor given above, the dissipation function for this system is $\overline{\Omega}_t=-1/t\int_0^t ds\beta_0J(s)V(s)F_c=-\beta_0\overline{(JV)}_tF_c$. Hence Eq. (3) with this expression yields[4]

$$\ln\left[\frac{\Pr(-\beta_0\overline{(JV)}_tF_c=A)}{\Pr(-\beta_0\overline{(JV)}_tF_c=-A)}\right]=At. \tag{6}$$

It is straightforward to show that the same expression is obtained when Nosé–Hoover constraints are applied to the pressure and temperature rather than Gaussian constraints; or if a combination of these types of thermostat is used.

In order to test the validity of Eq. (6) for the TFT we carried out computer simulations for a two-dimensional system with $N=98$ particles in a square unit cell with periodic boundary conditions. Note that the volume appearing in the general equations above will be the area of the unit cell. Both Lennard-Jones and SHREP potentials were used to model particle interactions. The SHREP potential is continuous and has first and second derivatives for all q, unlike the more commonly used truncated Lennard-Jones potential and therefore allowed longer time steps to be used in the simulation without introducing large numerical errors.[10] The temperature in both cases was $T=1.0$ and the number density was $n=0.4$. The pressure for the simulations performed using the Lennard-Jones potential was $p_0=0.968$ and the time step was 0.0001. For the SHREP potential, these values were $p_0=0.396$ and 0.001. Simulations were carried out with $F_c=0.05$ and 0.4. Nonequilibrium trajectories were periodically spawned from the initial isobaric–isothermal equilibrium trajectory and were propagated using the equations of motion (5). The lower field strength ($F_c=0.05$) was used for those simulations with transient lengths that approached or exceeded the Maxwell relaxation time, in order to facilitate the observation of antisegments in the presence of such long averaging times. The steady state version of Eq. (6) was also tested for the ESSFT and DSSFT with $N=98$, $T=1.0$, $n=0.4$, $p_0=0.968$, time step$=0.001$, $F_c=0.05$, and $t=16.0$. The SHREP potential was used to model interparticle interactions in the ESSFT and DSSFT simulations.

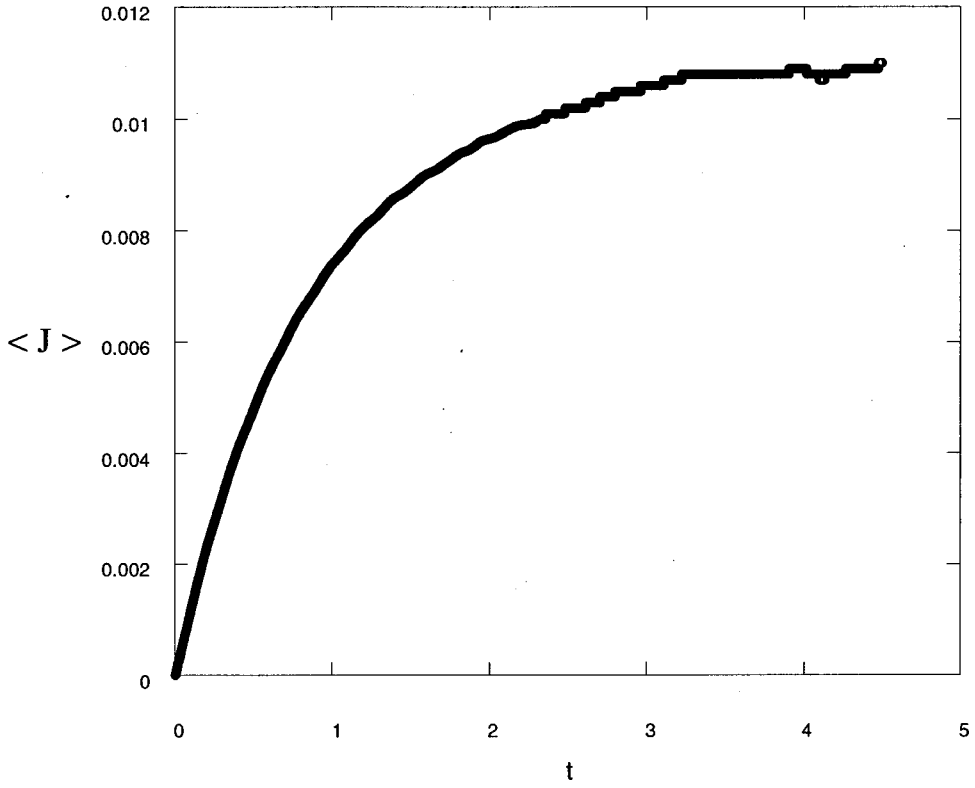

FIG. 1. A plot of the response of the ensemble average of the current density, $\langle J \rangle$, to the external field vs time for a calculation with the SHREP potential in two Cartesian dimensions, $N=98$, $T_0=1.0$, $n=0.4$, $p_0=0.396$, and $F_c=0.05$. The time of the simulation was $t=4.5$. Note that from the plot it may be ascertained that the Maxwell relaxation time is approximately $t=1$.

Figure 1 shows the ensemble averaged transient response of the dissipative flux to the applied field for a simulation using the SHREP potential. The Maxwell time for these systems is approximately 1.0. In Fig. 2, Eq. (6) is tested for the system where the particles are interacting via a Lennard-Jones potential and the trajectory segments are of length $t=1.0$. Figure 3 shows the results of the tests using the same equation but for the SHREP potential. Here the data for $t=3.5$ (shown as circles) and $t=4.5$ (shown as crosses) are plotted, by which time the system has already reached a steady state. If the FT works under isokinetic–isobaric dynamics, a line of unit slope will be obtained and clearly the FT is satisfied in all cases. Figure 4 shows the results of ESSFT (depicted with crosses) and DSSFT (depicted with

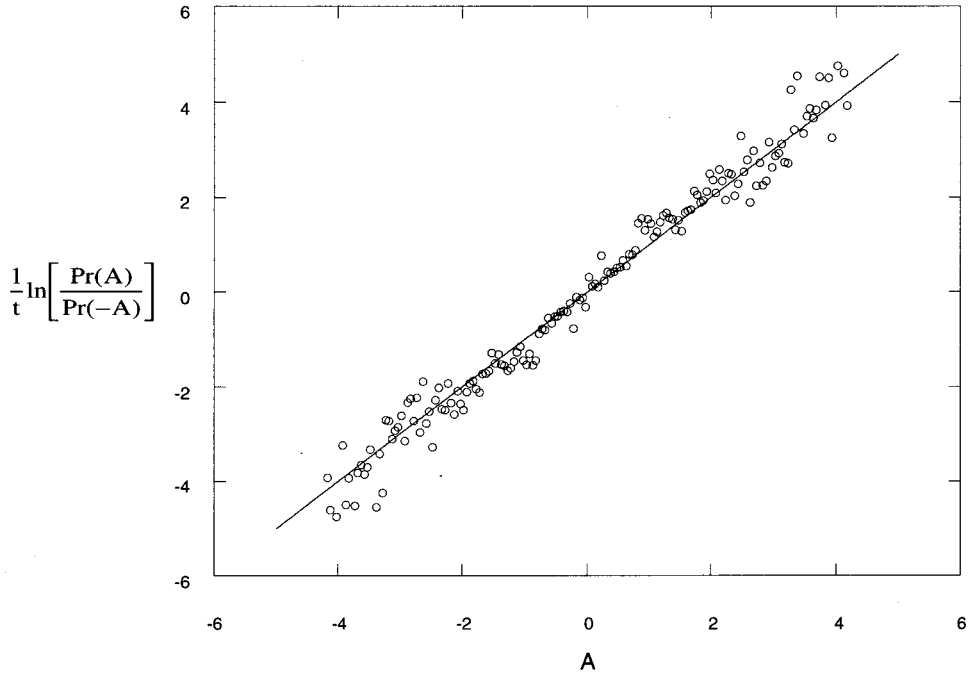

FIG. 2. A test of the TFT for an isobaric–isokinetic system that is given by Eq. (6). The value of $(1/t)\ln[\Pr(\bar{\Omega}_t=A)]/[\Pr(\bar{\Omega}_t=-A)]$ is plotted as a function of A for a system of $N=98$ particles in two Cartesian dimensions. The length of the nonequilibrium trajectory segments was $t=1.0$ (approximately equal to the Maxwell relaxation time). The particle interactions were modeled by a Lennard-Jones potential with a cutoff radius of 3.0, $T_0=1.0$, $n=0.4$, $p_0=0.968$. F_c for this simulation was 0.4. The FT given by Eq. (6) predicts the solid line shown on the plot, which has a slope of unity.

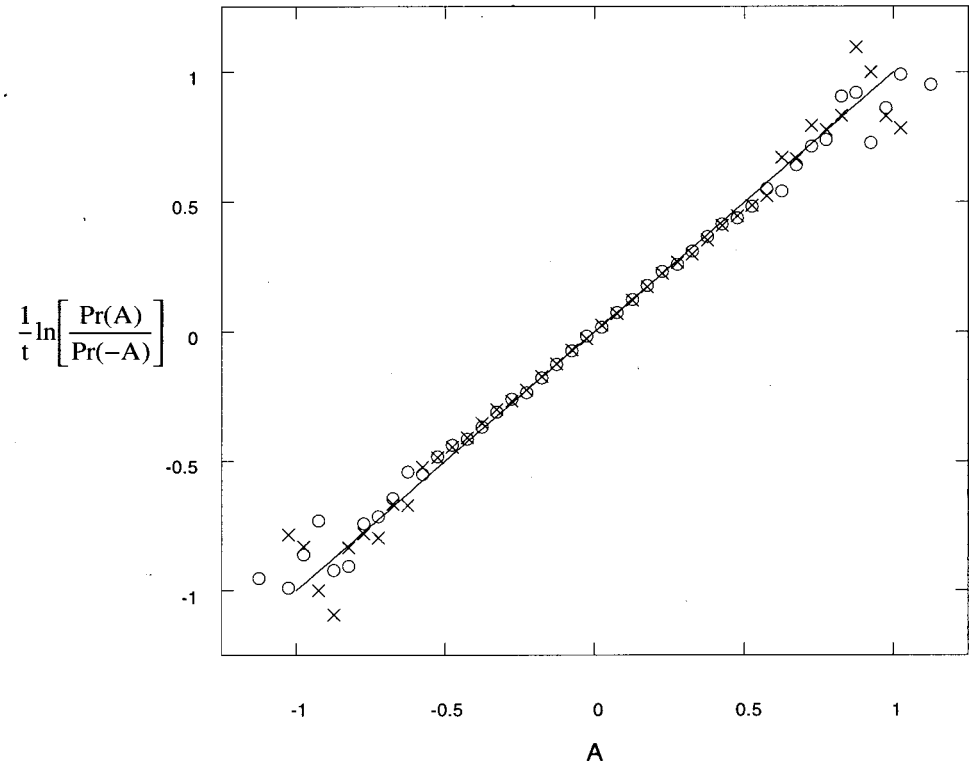

FIG. 3. A test of the TFT for an isobaric–isokinetic system that is given by Eq. (6). The value of $(1/t)\ln[\Pr(\overline{\Omega}_t=A)]/[\Pr(\overline{\Omega}_t=-A)]$ is plotted as a function of A for a system of $N=98$ particles in two Cartesian dimensions. Two sets of data are shown. The length of the nonequilibrium trajectory segments was $t=4.5$ (shown by crosses) and $t=3.5$ (shown by circles). Particle interactions were modelled by the SHREP potential with a cutoff radius of 1.125, $T_0=1.0$, $n=0.4$, $p_0=0.396$, and $F_c=0.05$. The FT predicts the solid line shown on the plot, which has a slope of unity.

circles) simulations with nonequilibrium trajectories of length $t=16$. For the ESSFT, longer nonequilibrium segments were necessary to facilitate obtaining averages of properties well past the Maxwell relaxation time. To test the ESSFT, an ensemble of trajectories was generated, and time-averaging was commenced 4 time units after the application of the field (i.e., time-averaging was carried out from $t=4.0$ to $t=20.0$). In order to test the DSSFT, a single steady state trajectory was divided into segments of length $t=16.0$. Error bars are shown for every point obtained from

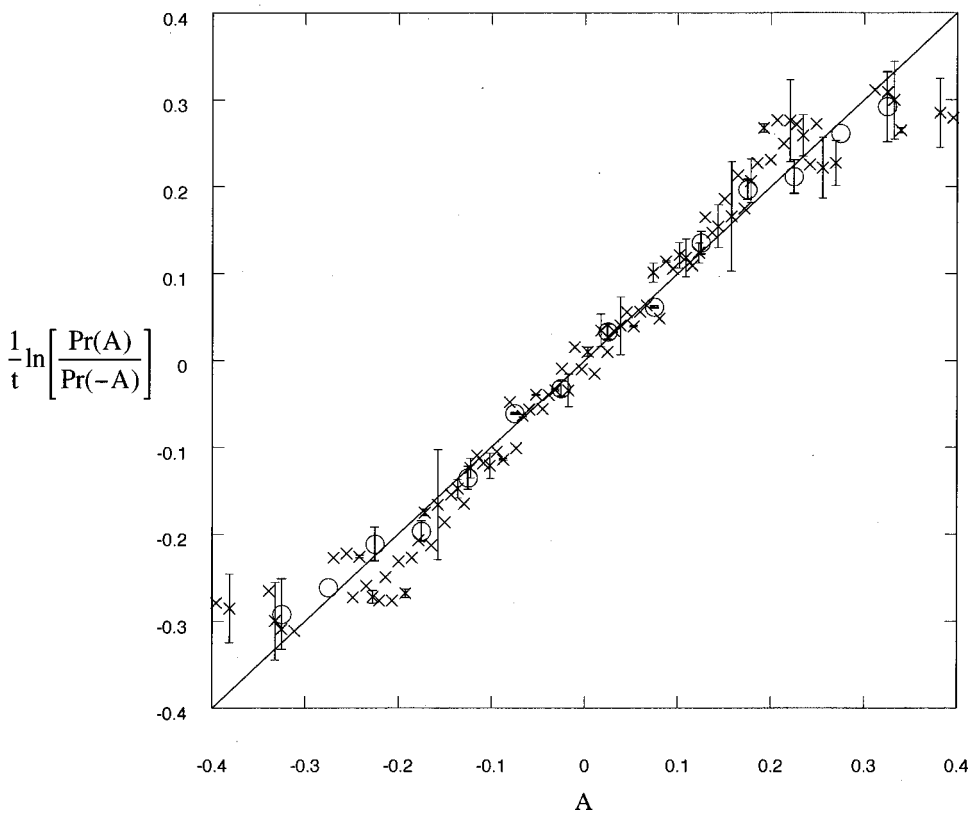

FIG. 4. A test of the ESSFT (crosses) and DSSFT (circles) given by the steady state version of Eq. (6). The value of $(1/t)\ln[\Pr(\overline{\Omega}_t=A)/\Pr(\overline{\Omega}_t=-A)]$ is plotted as a function of A for a system of $N=98$ particles in two Cartesian dimensions. The nonequilibrium trajectory segments are of length $t=16$. For the ESSFT, averages were taken over an ensemble of trajectories with time-averaging commencing 4.0 time units after the application of the field. The DSSFT trajectory segments were taken by dividing a single steady state trajectory into segments. In both cases, particle interactions were modeled by the SHREP potential with a cutoff radius of 1.125, $T_0=1.0$, $n=0.4$, $p_0=0.396$, and $F_c=0.05$. The FT predicts the solid line shown on the plot, which has a slope of unity. Error bars are shown for every point on the graph obtained from the DSSFT simulation, while only those for appoximately half of the points are shown for the ESSFT simulation.

the DSSFT simulation. For the ESSFT data, error bars are shown for only every second data point. In both cases, a slope of unity is expected and is observed, demonstrating adherence to both the ESSFT and DSSFT.

We have shown that the fluctuation theorem is satisfied under constant temperature and constant pressure conditions, which further verifies its validity. We have also found that the SHREP potential is a useful model potential for isobaric simulations when using a Gaussian barostat multiplier in the equations of motion, since the commonly used Lennard-Jones potential is more sensitive to fluctuations in the pressure. Simulations with a Lennard-Jones potential may still be used to verify the isothermal–isobaric form of the FT. The small time step necessary in this case, however, makes the SHREP potential much more suitable for such calculations.

The isothermal–isobaric FT, as with previous versions of the theorem, shows that as the size of the system and/or the averaging time increases, the probability that the Second Law of Thermodynamics will be obeyed increases exponentially.

The authors thank the Australian Research Council for support of this project. The Australian Partnership for Advanced Computing and the Supercomputer Facility of the Australian National University are acknowledged for computer time.

[1] D. J. Evans, E. G. D. Cohen, and G. P. Morriss, Phys. Rev. Lett. **71**, 2401 (1993).
[2] G. Gallavotti and E. G. D. Cohen, Phys. Rev. Lett. **74**, 2694 (1995).
[3] D. J. Evans and D. J. Searles, Phys. Rev. E **50**, 1645 (1994).
[4] D. J. Searles, G. Ayton, and D. J. Evans, AIP Conf. Proc. **519**, 271 (2000).
[5] D. J. Searles and D. J. Evans, J. Chem. Phys. **113**, 3503 (2000).
[6] D. J. Evans, D. J. Searles, and E. Mittag, Phys. Rev. E **63**, 051105 (2001).
[7] D. J. Searles and D. J. Evans, J. Chem. Phys. **112**, 9727 (2000).
[8] S. Hess and M. Kröger, Phys. Rev. E **61**, 4629 (2000).
[9] D. J. Evans and G. P. Morriss, *Statistical Mechanics of Nonequilibrium Liquids* (Academic, London, 1990).
[10] Note that the WCA potential is too sensitive to pressure fluctuations to allow a Gaussian barostat to function properly for time steps larger than ~0.0001.